doi:10.1006/jmbi.2000.3785 available online at http://www.idealibrary.com on IDEAL® *J. Mol. Biol.* (2000) **299**, 875–883

JMB

COMMUNICATION

The Role of Weak Protein-Protein Interactions in Multivalent Lectin-Carbohydrate Binding: Crystal Structure of Cross-linked FRIL

Thomas W. Hamelryck[1]*, Jeffrey G. Moore[2], Maarten J. Chrispeels[3], Remy Loris[1] and Lode Wyns[1]

[1]*Laboratorium voor Ultrastructuur, Vlaams Interuniversitair Instituut voor Biotechnologie, Vrije Universiteit Brussel Paardenstraat 65, B-1640, Sint-Genesius-Rode, Belgium*

[2]*Phylogix LLC, P.O. Box 6790 69 U.S. Route One Scarborough, ME 04074, USA*

[3]*Department of Biology University of California, San Diego, 9500 Gilman Drive, La Jolla, CA 92093-0116, USA*

**Corresponding author*

Binding of multivalent glycoconjugates by lectins often leads to the formation of cross-linked complexes. Type I cross-links, which are one-dimensional, are formed by a divalent lectin and a divalent glycoconjugate. Type II cross-links, which are two or three-dimensional, occur when a lectin or glycoconjugate has a valence greater than two. Type II complexes are a source of additional specificity, since homogeneous type II complexes are formed in the presence of mixtures of lectins and glycoconjugates. This additional specificity is thought to become important when a lectin interacts with clusters of glycoconjugates, e.g. as is present on the cell surface. The cryst1al structure of the Glc/Man binding legume lectin FRIL in complex with a trisaccharide provides a molecular snapshot of how weak protein-protein interactions, which are not observed in solution, can become important when a cross-linked complex is formed. In solution, FRIL is a divalent dimer, but in the crystal FRIL forms a tetramer, which allows for the formation of an intricate type II cross-linked complex with the divalent trisaccharide. The dependence on weak protein-protein interactions can ensure that a specific type II cross-linked complex and its associated specificity can occur only under stringent conditions, which explains why lectins are often found forming higher-order oligomers.

Keywords: X-ray crystallography; lectins; cross-linking; multivalent binding; protein-carbohydrate interactions

Lectins are proteins that bind carbohydrates in a reversible manner (Lis & Sharon, 1998). They are ubiquitous in nature and play a role in cancer, fertilization, immune response and signal transduction (Gabius & Gabius, 1997). Multivalent lectins can form cross-linked complexes with multivalent carbohydrate epitopes, which fall into two distinct types (for a review see Brewer, 1996). Linear type I cross-links, which are most often soluble, occur between a divalent lectin and a divalent carbohydrate (Weis *et al.*, 1992; Bourne *et al.*, 1994a). Non-linear two or three-dimensional type II cross-links, which are most often insoluble, occur when the lectins and/or carbohydrates involved have a valence greater than two (Dessen *et al.*, 1995; Wright & Hester, 1996; Olsen *et al.*, 1997; Cheng *et al.*, 1998; Lee *et al.*, 1998). Formation of a type II cross-linked complex confers additional specificity to a lectin, since homogeneous cross-linked complexes are formed even in the presence of mixtures of lectins and carbohydrates or glycoproteins (Bhattacharyya *et al.*, 1988, Gupta *et al.*, 1994, Brewer, 1996). This additional specificity is thought

Present address: T. W. Hamelryck, Institute for Molecular and Structural Biology, Århus University, Gustav Wieds Vej 10 C, DK-8000 Århus, Denmark.

Abbreviations used: CC, correlation coefficient; Con A, concanavalin A from *Canavalia ensiformis*; Con Br, concanavalin Br from *Canavalia brasiliensis*; DBL, *Dolichos biflorus* seed lectin; DB58, *Dolichos biflorus* stem-and-leaf lectin (58 kD); FRIL, Flt3 interacting lectin from *D. lablab*; GNA, *Galanthus nivalis* agglutinin; M3M6M, Man(α1-3)[Man(α1-6)]Man(α1-*O*-Me); M3, the (α1-3) linked Man residue of M3M6M; M6, the (α1-6) linked Man residue of M3M6M; NCS, non-crystallographic symmetry.

E-mail address of the corresponding author: thamelry@vub.ac.be

0022-2836/00/040875–9 $35.00/0

to become important when a lectin cross-links glycoconjugates on the cell surface, which often leads to signal transduction effects (Heldin, 1995).

FRIL (Flt3 receptor interacting lectin) is a Man/Glc binding legume lectin isolated from the seeds of *Dolichos lablab* (hyacinth bean) (Colucci *et al*., 1999; Mo *et al*., 1999). FRIL is a dimeric two-chain $(\alpha\beta)_2$ legume lectin with a molecular mass of 67 kDa. The sequence of FRIL has a high degree of similarity (78 %) to an earlier reported sequence of another dimeric two-chain Man/Glc-specific legume lectin (called DLL) isolated from a different *D. lablab* cultivar (Gowda *et al*., 1994). Evolutionarily, FRIL belongs to the Man/Glc-specific lectins isolated from the *Diocleae* and *Sophoreae* tribes, including Con A (52 % identity with FRIL), *Bowringia milbraedii* lectin (54 %), *Cladastris lutea* agglutinin (51 %) and *Sophora japonica* bark lectin (50 %) (Van Damme *et al*., 1998). Precipitation-inhibition studies indicate that FRIL has a preference for α-anomeric Man residues: Man(α1-3)[Man(α1-6)]Man(α1-*O*-Me) and Me-α-Man are respectively 4.1 and 3.6-fold better inhibitors of precipitation than Man (Mo *et al*., 1999).

FRIL is of considerable therapeutic interest because it maintains primitive hematopoietic progenitors in a quiescent state for two to four weeks *in vitro* (Colucci *et al*., 1999). The rapid proliferation and differentiation of these cells is a serious problem for their utilization in therapeutic treatment and scientific research. FRIL was crystallized in the presence of the trisaccharide Man(α1-3)[Man(α1-6)]Man(α1-*O*-Me) (M3M6M).

The FRIL monomer resembles a typical legume lectin monomer, i.e. a β-sandwich consisting of two large β-sheets and one small β-sheet. *In vivo*, the 264-residue FRIL monomer is proteolitically processed, resulting in two chains, named α (the C-terminal part) and β (the N-terminal part). Residues Ala1 to Asn113 of the β-chain are visible in the electron density analysis. For the α-chain, electron density is observed starting from Ser132 and ending at Asn248. No density is seen for the last 16 residues (Val249-Leu264) of the C terminus of the α-chain, which is likely due to a combination of flexibility and C-terminal truncation.

Although FRIL is a dimer in solution, the crystal structure here described reveals the presence of a Con A-type $(\alpha\beta)_4$ tetramer in the asymmetric unit (Figure 1(c)). Con A can be considered as a dimer of two canonical legume lectin dimers (Figure 1(a)), which is the quaternary structure adopted by the *Vicieae* lectin dimers (for a review, see Loris *et al*., 1998). Hence, FRIL is probably a canonical dimer (Figure 1(a)) in solution which can transiently form a Con A tetramer. However, it cannot be completely excluded that FRIL forms an alternative dimer in solution (Figure 1(b)), in analogy with the dimeric leguminous lectin DB58 (Hamelryck *et al*., 1999).

The interface between the two canonical dimers in the FRIL tetramer differs substantially from the equivalent interface in Con A. In FRIL, two distinct regions on the back β-sheet of the subunit are mainly involved in dimer-dimer contacts, including β-strands 4 and 5 (His181-Ser200) and a cluster of residues around the C terminus (Val64, Val65, Trp246 and Asn248). The same regions are also involved in the inter-dimer contacts in Con A, but a substantial number of additional contacts (17 residues in FRIL; 24 residues in Con A) are present. These extra contacts are made by Lys114, Val187, Ser108, Asn131, Glu192 and Thr196 in Con A. As a result, the total buried surface area (Table 1) is considerably lower for FRIL (1744 Å^2) than for Con A (2564 Å^2). In addition, only two ionizable residues are present at the interface in FRIL (His181 and Arg190) while there are seven in Con A (His51, Asp58, Arg60, Lys114, Lys116, His121 and Glu192). The charged residues in Con A are involved in salt bridges across the dimer-dimer interface and stabilize the Con A tetramer. These differences probably prevent the formation of a tightly associated Con A-type FRIL tetramer in solution, but still allow its formation in the crystal.

Each FRIL subunit in the asymmetric unit binds one non-reducing Man residue in the conserved monosaccharide binding site. Binding of Man in the monosaccharide binding site (Figure 2 and Table 2) is similar to Man binding by other Man/Glc specific legume lectins (Loris *et al*., 1998), involving four conserved residues (Asp86, Gly104, Tyr142, Asn144) and the monosaccharide specificity loop (Glu229-Asp230).

Both Con A and FRIL are Man/Glc-binding legume lectins. They differ, however, in their oligosaccharide-binding specificity. Con A has a 60-fold higher affinity for M3M6M than for Me-α-D-Man, and a 180-fold higher affinity for the pentasaccharide GlcNAc(β1-2)Man(α1-3)[GlcNAc(β1-2)Man(α1-

Table 1. Total contacts, hydrophobic contacts and hydrophylic contacts for FRIL and Con A

	Total contacts (Å^2)	Hydrophobic contacts (Å^2)	Hydrophilic contacts (Å^2)
Con A, Canonical dimer	2539 23 residues	1420 (56 %)	1119 (44 %)
FRIL, Canonical dimer	1991 22 residues	1065 (54 %)	916 (46 %)
Con A, Alternative dimer	2564 24 residues	1253 (49 %)	1311 (51 %)
FRIL, Alternative dimer	1744 17 residues	1062 (61 %)	672 (39 %)

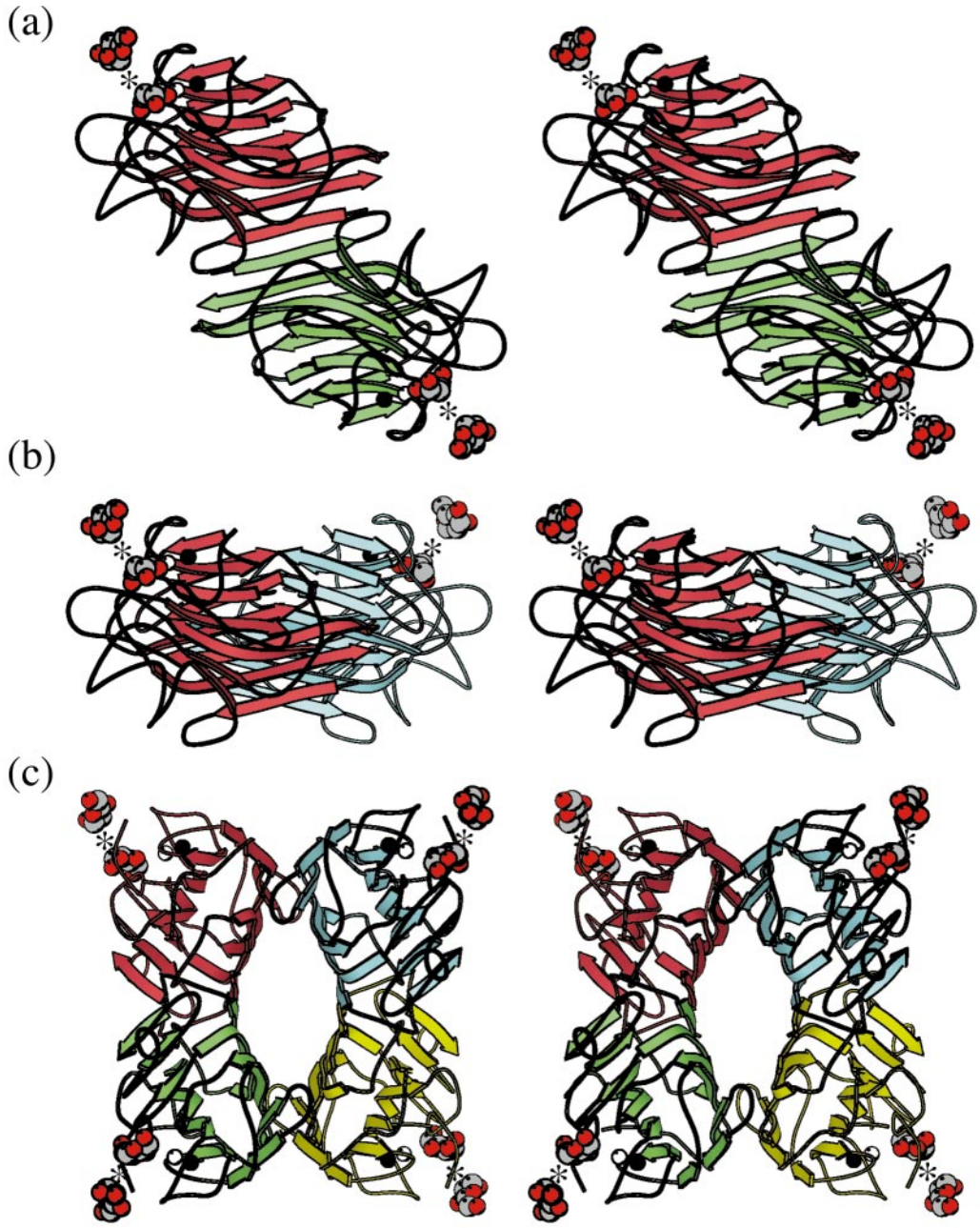

Figure 1. (a) Stereoview of the canonical FRIL dimer in complex with the M3M6M trisaccharide. Both subunits are shown in different colors. β-Strands are shown as arrows; Ca^{2+} are shown as white spheres; Mn^{2+} are shown as black spheres. The reducing Man residue is disordered in the crystal and was therefore not built into the structure. An asterisk indicates the approximate position of this Man residue. The visible Man residues are shown as CPK models (carbon atoms, gray, oxygen atoms, red). The view is perpendicular to the direction of the crystallographic 6_5-screw axis. (b) Stereoview of the alternative FRIL dimer in complex with the Man(α1-3)[Man(α1-6)]Man trisaccharide. The view is identical to the view in (a). β-Strands, metals, subunit colors and sugars as in (a). (c) Stereoview of the crystallographic Con A-like FRIL tetramer. The view is along the direction of the crystallographic 6_5-screw axis. β-Strands, metals, subunit colors and sugars as in (a) and (b).

6)]Man (Mandal *et al*., 1994). Comparison of the extended binding site of Con A with the corresponding region in FRIL indicates that Thr15 in Con A is replaced by Pro145 in FRIL. Thr15 O^{γ} is involved in a hydrogen bond with O3 of the (α1-3) linked Man residue in Con A, and its replacement in FRIL thus abolishes high-affinity binding of M3M6M. FRIL's fine specificity also differs from that of the Man/Glc binding *Vicieae* lectins, because FRIL lacks subsites for the Fuc(α1-6)GlcNAc disaccharide (Bourne *et al*., 1994b) and a Gal monosaccharide (Bourne *et al*., 1990).

The absence of a specific binding site for the complete M3M6M trisaccharide in FRIL allows it

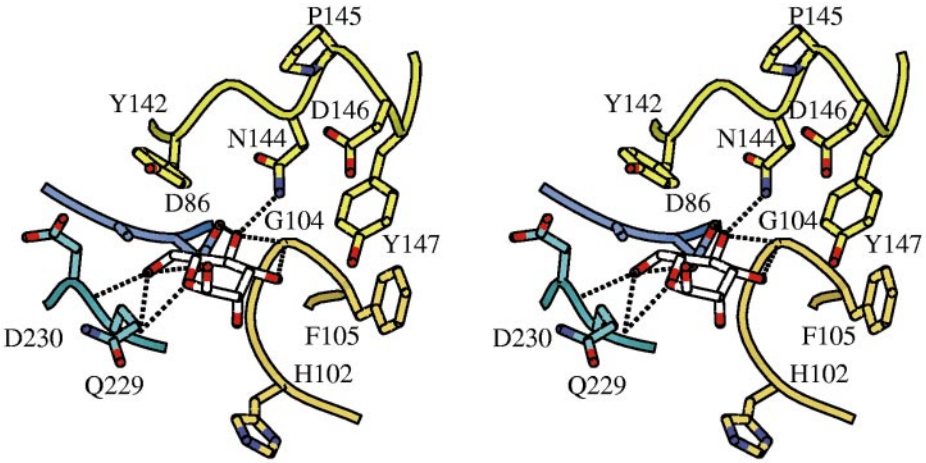

Figure 2. A view on the monosaccharide binding site of FRIL in complex with Man(α1-3)[Man(α1-6)]Man. The non-reducing Man residue in the monosaccharide binding site and the neighboring residues are shown as ball-and-stick models. The sugar-binding residues of FRIL belong to four different stretches, each shown in a different color. Nitrogen atoms are shown in blue; oxygen atoms in red. Hydrogen bonds between sugar and protein residues are shown as broken lines.

to cross-link two FRIL subunits (Figure 3). A study indicating that complex type sugars containing the M3M6M epitope do not precipitate Con A corroborates this (Bhattacharyya *et al.*, 1987). Sugars containing a GlcNAc bisected M3M6M epitope do precipitate Con A, because the GlcNAc moiety prevents the M3M6M moiety from binding in the extended binding site.

The trisaccharide is in a conformation that has a pseudo 2-fold symmetry axis running through the central Man residue which maps the outer (α1-6) and (α1-3) linked Man residues onto each other. In the crystal, this pseudo 2-fold axis coincides with a true crystallographic 2-fold axis. The electron density of the central Man residue is thus averaged over two orientations with half occupancy. Since the averaged electron density for the central Man residue was difficult to interpret, it was not built into the structure. The density in the conserved monosaccharide binding site thus belongs to an (α1-3) and an (α1-6) linked Man residue, each bound with half occupancy. A similar phenomenon has been reported for the crystal structures of type II cross-links of soybean agglutinin (Dessen *et al.*, 1995; Olsen *et al.*, 1997) and snowdrop agglutinin (Wright & Hester, 1996).

Table 2. Van der Waals contacts (<4.0 Å) between the Man bound in the monosaccharide binding site and FRIL

C1	Gln229 (3)
C4	Asp86 (1), Gly103 (1), Gly104 (1)
C5	Asp86 (1), Tyr142 (2), Gln229 (1)
C6	Ala85 (1), Asp86 (2), Tyr142 (4), Gln229 (1), Asp230 (1)
O2	Gly228 (1), Gly229 (1)
O3	Gly103 (1), Gly104 (1)
O4	Asp86 (3), Gly103 (2), Gly104 (2), Tyr142 (2), Asn144 (3)

The number of contacts is shown between brackets.

The cross-linked canonical FRIL dimers are organized in a helical structure, with six dimers per turn (Figure 3(a)). The axis of the helix coincides with the 6_5-screw axis along the *c*-axis of the cell. The helix has a pitch of 310 Å, which corresponds to the length of the *c*-axis, and a large central pore with a diameter of approximately 90 Å.

Each 6_5-screw axis forms the center of four such helices, which together form a quadruple superhelix (Figure 3(b)). Each helix consists solely of AB dimers (helix H_{AB}) or CD dimers (helix H_{CD}), and the quadruple superhelix is formed in the order H_{AB}-H_{CD}-H_{CD}-H_{AB}. The contact between the helices in this quadruple superhelix is limited: the only contacts are three Van der Waals contacts between Ser38 D (O^{γ}) and Ala39 D (N, C^{α} and C^{β}) from two neighboring H_{CD} helices. There are no contacts between the H_{AB} helices in the superhelix, nor between the H_{AB} and H_{CD} helices. The organization of the helices in a quadruple superhelix accounts for the translational symmetry shown by the native Patterson map (see Materials and Methods).

In the crystal, each quadruple superhelix makes extensive contacts with six other superhelices (Figure 3(c)): each canonical FRIL dimer in one superhelix forms a Con A-type tetramer with a canonical FRIL dimer from another superhelix. The canonical FRIL dimers in the H_{CD} helices always associate with the canonical dimers in the H_{AB} helices and *vice versa*, thereby forming the Con A tetramer (comprising monomers A, B, C and D) that forms the asymmetric unit. The cross-linked structure is thus not only dependent on the cross-linking sugar, but also on the formation of a crys-

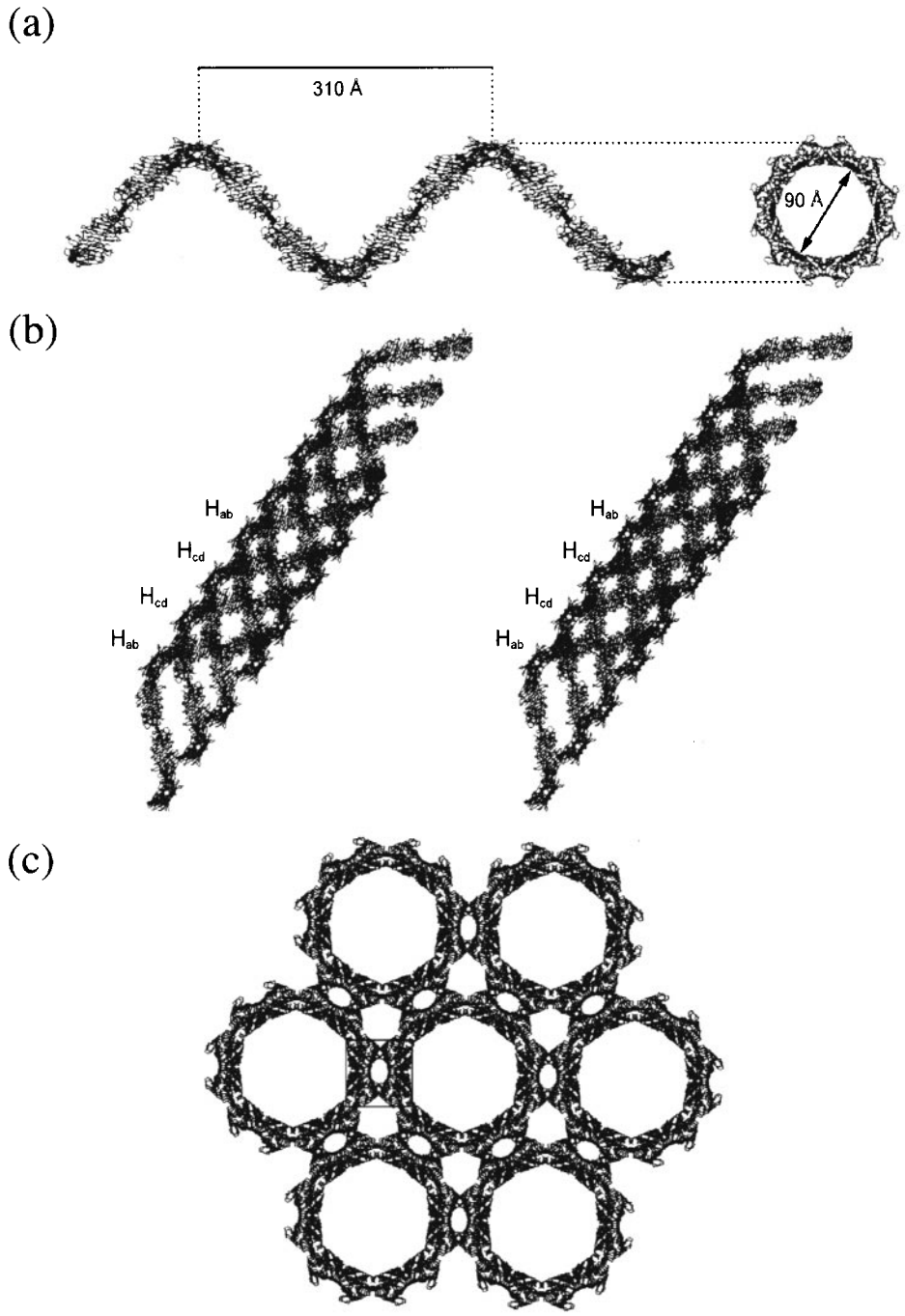

Figure 3. (a) Single helix of cross-linked canonical FRIL dimers. The sugar is shown as a black CPK model, the FRIL dimer is represented as a C^{α}-trace. The view is perpendicular to the helical axis, which coincides with the crystallographic 6_5-screw axis. The pitch of the helix is indicated. The right part of the Figure shows a view on the helix along the helical axis. The radius of the central pore is indicated. (b) Stereoview of the quadruple superhelix of cross-linked canonical FRIL dimers. (c) A view on the crystal packing of FRIL along the helical axis. One central quadruple superhelix is shown, together with its six neighboring superhelices. Each canonical FRIL dimer from one superhelix forms a Con A tetramer (one Con A tetramer is boxed in the Figure) with a dimer from a neighboring superhelix.

tallographic Con A-type tetramer. The FRIL cross-link differs from previously described cross-linked complexes because it depends on the formation of an oligomer that is not observed in solution for the native protein.

It has been shown that lectins are able to discriminate between different glycoconjugates by the formation of type II cross-linked lattices (Brewer, 1996). Cross-linking of cell surface receptors is an important mechanism of signal transduction

(Heldin, 1995). The FRIL crystal structure indicates that the formation of a type II cross-linked lattice can depend on the formation of an oligomer that is not or only transiently present in solution. In the case of FRIL, the formation of the cross-linked lattice depends on the formation of a Con A-type tetramer from two dimers. The dependence of type II lattice formation on the oligomerization of a lectin can give rise to subtle regulation mechanisms of lectin function. The formation of the oligomer and the associated type II lattice can depend on the local lectin/glycoconjugate concentration, pH conditions or the accessibility of the oligomer interface when a glycoconjugate is bound.

Examples of higher-order multimer formation in lectin crystal structures are ubiquitous. The dimeric leguminous lectin DB58 forms a DBL-like tetramer (Hamelryck *et al*., 1999). Con A, which is a tetramer above pH 6.5, and dissociates into dimers below pH 6.5, crystallizes as a tetramer at pH 5.0 (Bouckaert *et al*., 1995). The monomeric spermadhesin aSFP forms a dimer in the crystal that resembles a canonical legume lectin dimer (Romao *et al*., 1997). The heterodimeric spermadhesin PSP-I/PSP-II forms a heterotetramer that resembles the peanut agglutinin tetramer (Varela *et al*., 1997). The monomeric galectin-7 forms a dimer that somewhat resembles the dimeric leguminous lectin Ecorl (Leonidas *et al*., 1998). The tetrameric jacalin-related plant lectin heltuba forms a donut-shaped octamer (Bourne *et al*., 1999). In addition, a chemically modified, dimeric form of Con A crystallizes as a tetramer in two different cross-linked complexes (Dimick *et al*., 1999).

The formation of higher-order multimers has also been observed for lectins in solution. Galectin-1 isolated from Chinese hamster ovary cells undergoes a concentration-dependent monomer-dimer equilibrium (Cho & Cummings, 1995). Monomeric galectin-3 also forms higher-order multimers in solution or bound to immobilized ligands, which is dependent on its N or C-terminal regions (Hsu *et al*., 1992; Mehul *et al*., 1994; Yang, *et al*., 1998; Seetharaman *et al*., 1998). Calvete *et al*. (1999) found that leguminous lectins from the *Diocleinae* subtribe (which includes Con A and Con Br) show different pH-dependent dimer-tetramer equilibria, and suggest that these differences are responsible for the different biological activities of these lectins.

The described mechanism above of lattice formation by weakly associated oligomers provides an explanation for the frequent occurrence of higher order oligomerization in the different lectin families.

Materials and Methods

Purification and crystallization

D. lablab seeds were purchased from Stokes Seeds (Buffalo, NY, USA). Purification of FRIL from these seeds has been described (Mo *et al*., 1999). Suitable crystallization conditions were screened using the hanging drop method at room temperature. The hanging drop consisted of 5 μl FRIL solution (4.3 mg/ml), 5 μl of the bottom solution and 1 μl Man(α1-3)[Man(α1-6)]Man(α1-*O*-Me) solution (90 mM). The drops were equilibrated against 0.5 ml of the bottom solution at 20 °C. Between ten and 20 small crystals (maximum dimension 0.1 mm) were found with a bottom solution consisting of 20 % PEG 8000, 0.1 M Na Cacodylate (pH 6.5), 0.2 M $(NH_4)_2SO_4$. Optimizing the PEG 8000 concentration to 11 % led to the growth of one to three large (0.4 mm in all directions) crystals with perfect habit per drop. These crystals were mounted in boro-silicate capillaries and used for data collection.

Data collection, processing and analysis

The crystals were hexagonal (spacegroup $P6_522$ or $P6_122$) and diffracted to a resolution of 3.5 Å. Data were collected from six different crystals. Three crystals were used for data collection at the CCLRC Daresbury synchrotron facility (station 9.5), using X-rays with a wavelength of 0.92 Å (one crystal, 43 frames) or 1.1 Å (two crystals, 22 frames). The oscillation range was 0.8°. Three crystals were used for data collection at the DESY synchrotron facility, Hamburg (station BW7A), using X-rays with a wavelength of 0.95 Å (66 frames). The oscillation range was 0.5°. The detector used was a MAR image plate in both cases. Indexing and merging of the data was done with the HKL package (Otwinowski & Minor 1997). Intensities were transformed to structure factor amplitudes with the CCP4 (CCP4, 1994) program TRUNCATE. Table 3 shows the relevant crystal and diffraction statistics. Calculating and plotting of a native Patterson map with the CCP4 programs FFT and NPO revealed two unique peaks on the *z*-axis (at fractional positions 0, 0, 1/4 and 0, 0, 1/2) in addition to the origin peaks, indicating the presence of translational symmetry along the *z*-direction.

Molecular replacement

The structure was solved using the molecular replacement method with the CCP4 program AMoRe (Navaza, 1994). Molecular replacement was done in the two possible space groups, i.e. $P6_122$ and $P6_522$. For the rotation search, data between 19.0 and 4.0 Å were used, for the translation search, data between 8.0 and 3.0 Å were used.

Since FRIL is a dimer in solution, molecular replacement was first unsuccessfully attempted using a canonical legume lectin dimer (the canonical dimer present in Con A; PDB entry 1CVN) as phase model. Subsequently, a complete Con A tetramer (PDB entry 1CVN) with full 222 symmetry was tried as phase model, since FRIL has high level of sequence identity (52 %) with Con A. The rotation search yielded a single peak (peak height = 38 σ). The translation search readily yielded one solution (CC = 63.5 %, *R*-factor = 46.6 %). Inspection of the crystal packing showed no sterical clashes and reasonable crystal contacts. The asymmetric unit, containing two canonical dimers that form a Con A-type tetramer, can also be represented as two canonical dimers related by a translation of 85 Å, which is in accordance with the observed presence of translational symmetry along the *z*-axis (see above). A molecular replacement attempt performed with the Con A tetramer as a model in space group $P6_122$ did not result in any reasonable solution, thereby confirming the space group to be $P6_522$.

Table 3. Statistics of crystallographic data and quality of the structures

Space group	$P6_522$
A. *Unit cell parameters*	
a, *b*, *c* (Å)	151.36; 151.36; 309.88
Contents of asymmetric unit	Two FRIL dimers
Resolution (Å)	20.0-3.5
$I/\sigma I$ ($I/\sigma I$ last shell; 3.62-3.5 Å)	11.3 (4.8)
R_{sym} (%)[a]	15.9
Completeness (%)	99.4
Number of reflections measured	257,389
Number of unique reflections	26,919
R_{cryst} [b], R_{free} (%)[c]	23.2, 25.2
rmsd ideal bond length (Å)	0.008
rmsd ideal impropers (deg.)	0.91
rmsd ideal dihedrals (deg.)	26.9
rmsd ideal bond angles (deg.)	1.6
B. *Ramachandran plot quality (%)*	
Most favored	78.2
Additionally allowed	21.3
Generously allowed	0.5
Forbidden	0.0

[a] $R_{merge} = \Sigma_{hkl}\Sigma_I|\langle I_{hkl}\rangle - I_{hkl}|/\Sigma_{hkl}\Sigma_I I_{hkl}$.
[b] $R_{cryst} = \Sigma_{hkl}|F_{hkl,o} - F_{hkl,c}|/\Sigma F_{hkl,o}$, where $F_{hkl,o}$ and $F_{hkl,c}$ are the amplitudes of the observed and calculated structure factors, respectively.
[c] $R_{free} = R_{cryst}$ value calculated with 10% of the reflections, not included in the refinement.

Inspecting the crystal packing of the FRIL dimers reveals why the crystals only diffract to 3.5 Å resolution, despite their large size (0.4 mm in all directions) and perfect habit. The crystals have a very high solvent content (70%) and contain very large (90 Å diameter) solvent channels, which indicates that the 3.5 Å resolution limit is probably the high-resolution limit for this crystal form.

Refinement and model building

The FRIL sequence was submitted to the SWISS-MODEL service for an automated modeling procedure (Peitsch, 1996) based on the Con A structure (PDB entry 1CVN). Loop regions in the model that were different from the Con A structure were removed prior to refinement. The structure was refined with the program CNS (Brünger *et al*., 1998) against a maximum likelihood target function (target function *mlf*). No σ cut-off was used during the refinement. Throughout the refinement, a real space bulk solvent model and an overall anisotropic *B*-factor correction was used. Strict positional NCS was imposed between the four subunits in the asymmetric unit, in view of the low resolution (3.5 Å). In addition, the φ and ψ angles of residues belonging to the conserved anti-parallel β-sheets (stretches 1-8, 17-22, 47-52, 62-74, 86-94, 134-140, 153-159, 165-169, 176-185, 189-196, 202-208 and 217-226) were restrained to −139.0° and 135.0°, respectively.

A rigid body refinement of the four FRIL subunits was performed, first against data between 20.0 and 5.5 Å, then against data between 20.0 and 4.5, and finally between 20.0 and 3.5 Å. Thereafter, a grouped *B*-factor refinement (one *B*-factor for each subunit) was performed. During the rest of the refinement, individual *B*-factors were refined with heavy restraints between the *B*-factors of side and main-chain atoms (target rms = 0.7 and 0.5 $Å^2$, respectively). Torsion angle refinement (start temperature 3500 K, "slowcool" protocol) and Powell conjugate gradient minimization were used for positional refinement.

In the beginning of the refinement, NCS-averaged and bulk solvent-corrected electron density maps were computed with the program DM (Cowtan & Main, 1993), using reflection weights generated with the program SIGMAA (Read, 1986). Afterwards, NCS-averaged maps were calculated with CNS using the "sigmaa" option. Model building was performed with the program TURBO (Roussel & Cambillau, 1989).

Figures and analysis

The quality of the structure was checked with PROCHECK (Laskowski *et al*., 1993). Van der Waals contacts (<4 Å) were determined with the CCP4 program (CCP4, 1994) CONTACT. Contact surfaces were calculated with ICM (Cardozo *et al*., 1995). Figures 1 and 2 were made with BOBSCRIPT (Esnouf, 1997). Figure 3, was made with RASMOL (Sayle & Milner-White, 1995).

Accession numbers

Atomic coordinates and structure factors have been submitted to the RCSB Protein Data Bank, and are available under entry codes 1QMO and R1QMOSF, respectively.

Acknowledgments

The authors thank Yves Geunes for excellent computer assistance. This work was supported by the Vlaams Interuniversitair Instituut voor Biotechnologie (V.I.B.). R.L., and T.W.H. are postdoctoral fellows of the Fonds voor Wetenschappelijk Onderzoek (F.W.O.).

References

Bhattacharyya, L., Haraldsson, M. & Brewer, C. F. (1987). Concanavalin A interactions with asparagine-linked glycopeptides. Bivalency of bisected complex type oligosaccharides. *J. Biol. Chem.* **262**, 1294-1299.

Bhattacharyya, L., Khan, M. I. & Brewer, C. F. (1988). Interactions of concanavalin A with asparagine-linked glycopeptides: formation of homogeneous cross-linked lattices in mixed precipitation systems. *Biochemistry*, **27**, 8762-8767.

Bouckaert, J., Loris, R. & Wyns, L. (1995). Change of the crystal space group and of the oligomeric structure as a function of metal ion binding and pH. In *Lectins: Biology, Biochemistry, Clinical Biochemistry* (Van Driessche, E. & Bøg-Hansen, T. C., eds), vol. 11, pp. 50-60. Textop, Hellerup, Denmark.

Bourne, Y., Rougé, P. & Cambillau, C. (1990). X-ray structure of a (α-Man(1-3)β-Man(1-4)GlcNAc)-lectin complex at 2.1-Å resolution. The role of water in sugar-lectin interaction. *J. Biol. Chem.* **265**, 18161-18165.

Bourne, Y., Bolgiano, B., Liao, D. I., Strecker, G., Cantau, P., Herzberg, O., Feizi, T. & Cambillau, C. (1994a). Crosslinking of mammalian lectin (galectin-

1) by complex biantennary saccharides. *Nature Struct. Biol.* **12**, 863-870.

Bourne, Y., Mazurier, J., Legrand, D., Rougé, P., Montreuil, J., Spik, G. & Cambillau, C. (1994b). Structures of a legume lectin complexed with the human lactotransferrin N2 fragment, and with an isolated biantennary glycopeptide: role of the fucose moiety. *Structure,* **2**, 209-219.

Bourne, Y., Zamboni, V., Barre, A., Peumans, W. J., Van Damme, E. J. M. & Rougé, P. (1999). *Helicanthus tuberosus* lectin reveals a widespread scaffold for mannose-binding lectins. *Structure,* **7**, 1473-1482.

Brewer, C. F. (1996). Multivalent lectin-carbohydrate cross-linking interactions. *Chemtracts Biochem. Mol. Biol.* **6**, 165-179.

Brünger, A. T., Adams, P. D., Clore, G. M., DeLano, W. L., Gros, P., Grosse-Kunstleve, R. W., Jiang, J. S., Kuszewski, J., Nilges, M., Pannu, N. S., Read, R. J., Rice, L. M., Simonson, T. & Warren, G. L. (1998). Crystallography and NMR system: a new software suite for macromolecular structure determination. *Acta Crystallog. sect. D,* **54**, 905-921.

Calvete, J. J., Thole, H. H., Raida, M., Urbanke, C., Romero, A., Grangeiro, T. B., Ramos, M. V., Almeida da Rocha, I. M., Guimarãs, F. N. & Cavada, B. S. (1999). Molecular characterization and crystallization of *Diocleinae* lectins. *Biochim. Biophys. Acta,* **1430**, 367-375.

Cardozo, T., Totrov, M. & Abagyan, R. (1995). Homology modeling by the ICM method. *Proteins: Struct. Funct. Genet.* **23**, 403-414.

Cheng, W., Bullitt, E., Bhattacharyya, L., Brewer, C. F. & Makowski, L. (1998). Electron microscopy and X-ray diffraction studies of *Lotus tetragonolobus* A isolectin cross-linked with a divalent Lewis^x oligosaccharide, an oncofetal antigen. *J. Biol. Chem.* **273**, 35016-35022.

Cho, M. & Cummings, R. D. (1995). Galectin-1, a β-galactoside-binding lectin in Chinese hamster ovary cells. *J. Biol. Chem.* **270**, 5198-5206.

Collaborative Computational Project No. 4 (1994). The CCP4 suite: programs for protein crystallography. *Acta Crystallog. sect. D,* **50**, 760-763.

Colucci, G., Moore, J. G., Feldman, M. & Chrispeels, M. J. (1999). cDNA cloning of FRIL, a lectin from *Dolichos lablab*, that preserves hematopoietic progenitors in suspension culture. *Proc. Natl Acad. Sci. USA,* **96**, 646-650.

Cowtan, K. D. & Main, P. (1993). Improvement of macromolecular electron-density maps by the simultaneous application of real and reciprocal space constraints. *Acta Crystallog. sect. D,* **49**, 148-157.

Dessen, A., Gupta, D., Sabesan, S., Brewer, F. & Sacchettini, J. C. (1995). X-ray crystal structure of the soybean agglutinin cross-linked with a biantennary analog of the blood group I carbohydrate antigen. *Biochemistry,* **34**, 4933-4942.

Dimick, S. M., Powell, S. C., McMahon, S. A., Moothoo, D. N., Naismith, J. H. & Toone, E. J. (1999). On the meaning of affinity: cluster glycoside effects and concanavalin A. *J. Am. Chem. Soc.* **121**, 10286-10296.

Esnouf, R. M. (1997). An extensively modified version of MolScript that includes greatly enhanced coloring capabilities. *J. Mol. Graphics,* **15**, 132-134.

Gowda, L. R., Savithri, H. S. & Rao, D. R. (1994). The complete primary structure of a unique mannose/glucose-specific lectin from field bean (*Dolichos lablab*). *J. Biol. Chem.* **269**, 18789-18793.

Gupta, D. & Brewer, C. F. (1994). Homogeneous aggregation of the 14-kDa β-galactoside specific vertebrate lectin complex with asialofetuin in mixed systems. *Biochemistry,* **33**, 5526-5530.

Gabius, H. J. & Gabius, S. (1997). *Glycosciences, Status and Perspectives*, Chapman & Hall, Weinheim.

Hamelryck, T. W., Loris, R., Bouckaert, J., Dao-Thi, M. H., Strecker, G., Imberty, A., Fernandez, E., Wyns, L. & Etzler, M. E. (1999). Carbohydrate binding, quaternary structure and a novel hydrophobic binding site in two legume lectin oligomers from *Dolichos biflorus*. *J. Mol. Biol.* **286**, 1161-1177.

Heldin, C. H. (1995). Dimerization of cell surface receptors in signal transduction. *Cell,* **80**, 213-223.

Hsu, D. K., Zuberi, R. & Liu, F. T. (1992). Biochemical and biophysical characterization of human recombinant IgE-binding protein, an S-type animal lectin. *J. Biol. Chem.* **267**, 14167-14174.

Laskowski, R. A., MacArthur, M. W., Moss, D. S. & Thornton, J. M. (1993). PROCHECK: a program to check the stereochemical quality of protein structures. *J. Appl. Crystallog.* **26**, 283-291.

Lee, X., Thompson, A., Zhang, Z., Ton-that, H., Biesterfeldt, J., Ogata, C., Xu, L., Johnston, R. A. & Young, N. M. (1998). Structure of the complex of *Maclura pomifera* agglutinin and the T-antigen disaccharide, Galβ1,3GalNAc. *J. Biol. Chem.* **273**, 6312-6318.

Leonidas, D. D., Vatzaki, E. H., Vorum, H., Celis, J. E., Madsen, P. & Acharya, K. R. (1998). Structural basis for the recognition of carbohydrates by human galectin-7. *Biochemistry,* **37**, 13930-13940.

Lis, H. & Sharon, N. (1998). Lectins: carbohydrate-specific proteins that mediate cellular recognition. *Chem. Rev.* **98**, 637-674.

Loris, R., Hamelryck, T., Bouckaert, J. & Wyns, L. (1998). Legume lectin structure. *Biochem. Biophys. Acta,* **1383**, 9-36.

Mandal, D. K., Kishore, N. & Brewer, C. F. (1994). Thermodynamics of lectin-carbohydrate interactions. Titration microcalorimatery measurements of the binding of *N*-linked carbohydrates and ovalbumin to concanavalin A. *Biochemistry,* **33**, 1149-1156.

Mehul, B., Bawumia, S., Martin, S. R. & Hughes, R. C. (1994). Structure of baby hamster kidney carbohydrate-binding protein CBP30, an S-type animal lectin. *J. Biol. Chem.* **269**, 18250-18258.

Mo, H., Meah, Y., Moore, J. G. & Goldstein, I. J. (1999). Purification and characterization of *Dolichos lablab* lectin. *Glycobiology,* **9**, 173-179.

Navaza, J. (1994). AMoRe: an automated package for molecular replacement. *Acta Crystallog. sect. A,* **50**, 157-163.

Olsen, L. R., Dessen, A., Gupta, D., Sabesan, S., Sacchettini, J. & Brewer, C. F. (1997). X-ray crystallographic studies of unique cross-linked lattices between four isomeric biantennary oligosaccharides and soybean agglutinin. *Biochemistry,* **36**, 15073-15080.

Otwinowski, Z. & Minor, W. (1997). Processing of X-ray diffraction data collected in oscillation mode. *Methods Enzymol.* **276**, 307-326.

Peitsch, M. C. (1996). ProMod and Swiss-Model: Internet-based tools for automated comparative protein modelling. *Biochem. Soc. Trans.* **24**, 274-279.

Read, R. J. (1986). Improved fourier coefficients for maps using phases from partial structures with errors. *Acta Crystallog. sect. A,* **42**, 140-149.

Romao, M. J., Kölln, I., Dias, J. M., Carvalho, A. L., Romero, A., Varela, P. F., Sanz, L., Töpfer-Petersen, E. & Calvete, J. J. (1997). Crystal structure of acidic seminal fluid protein (aSFP) at 1.9 Å resolution: a bovine polypeptide of the spermadhesin family. *J. Mol. Biol.* **274**, 650-660.

Roussel, A. & Cambillau, C. (1989). TURBO. In *Silicon Graphic Geometry Partner Directory*, p. 71, Silicon Graphics, Mountain View, CA, USA.

Sayle, R. A. & Milner-White, E. J. (1995). RASMOL: biomolecular graphics for all. *Trends Biochem. Sci.* **20**, 374-.

Seetharaman, J., Kanigsberg, A., Slaaby, R., Leffler, H., Barondes, S. H. & Rini, J. M. (1998). X-ray crystal structure of the human galectin-3 carbohydrate recognition domain at 2.1-Å resolution. *J. Biol. Chem.* **273**, 13047-13052.

Van Damme, E., Peumans, W. J., Barre, A. & Rougé, P. (1998). Plant lectins: a composite of several distinct families of structurally and evolutionary related proteins with diverse biological roles. *Crit. Rev. Plant Sci.* **17**, 575-692.

Varela, P. F., Romero, A., Sanz, L., Romao, M. J., Töpfer-Petersen, E. & Calvete, J. J. (1997). The 2.4 Å resolution crystal structure of boar seminal plasma PSP-I/PSP-II: a zona pellucida-binding glycoprotein heterodimer of the spermadhesin family built by a CUB domain architecture. *J. Mol. Biol.* **274**, 635-649.

Wright, C. S. & Hester, G. (1996). The 2.0 Å structure of a cross-linked complex between snowdrop lectin and a branched mannopentaose: evidence for two unique binding modes. *Structure,* **4**, 1339-1352.

Weis, W. I., Drickamer, K. & Hendrickson, W. A. (1992). Structure of a C-type mannose-binding protein complexed with an oligosaccharide. *Nature,* **360**, 127-134.

Yang, R. Y., Hill, P. N., Hsu, D. K. & Liu, F. T. (1998). Role of the carboxyl-terminal lectin domain in self-association of galectin-3. *Biochemistry,* **37**, 4086-4092.

Edited by R. Huber

(Received 10 January 2000; received in revised form 5 April 2000; accepted 5 April 2000)